

Strain-Induced Room-Temperature Ferromagnetic Semiconductors with Large Anomalous Hall Conductivity in Two-Dimensional $\text{Cr}_2\text{Ge}_2\text{Se}_6$

Xue-Juan Dong¹, Jing-Yang You¹, Bo Gu^{2,3,*} and Gang Su^{1,2,3†}

¹ *School of Physical Sciences, University of Chinese Academy of Sciences, Beijing 100049, China*

² *Kavli Institute for Theoretical Sciences, and CAS Center for Excellence in Topological Quantum Computation, University of Chinese Academy of Sciences, Beijing 100190, China*

³ *Physical Science Laboratory, Huairou National Comprehensive Science Center, Beijing 101400, China*

(Dated: March 17, 2022)

By density functional theory calculations, we predict a stable two-dimensional (2D) ferromagnetic semiconductor $\text{Cr}_2\text{Ge}_2\text{Se}_6$, where the Curie temperature T_c can be dramatically enhanced beyond room temperature by applying a few percent strain. In addition, the anomalous Hall conductivity in 2D $\text{Cr}_2\text{Ge}_2\text{Se}_6$ and $\text{Cr}_2\text{Ge}_2\text{Te}_6$ is predicted to be comparable to that in ferromagnetic metals of Fe and Ni, and is an order of magnitude larger than that in diluted magnetic semiconductor Ga(Mn,As). Based on superexchange interactions, the enhanced T_c in 2D $\text{Cr}_2\text{Ge}_2\text{Se}_6$ by strain can be understood by the decreased energy difference between $3d$ orbitals of Cr and $4p$ orbitals of Se. Our finding highlights the microscopic mechanism to obtain the room temperature ferromagnetic semiconductors by strain.

I. INTRODUCTION

Combining magnetism and semiconductor enables the development of magnetic semiconductors, a promising way to realize spintronic applications based on use of both charge and spin degrees of freedom in electronic devices [1, 2]. The highest Curie temperature of the most extensively studied magnetic semiconductor (Ga,Mn)As has been $T_c = 200$ K [3], still far below room temperature. The room temperature ferromagnetic semiconductors are highly required by applications. Recent advances in magnetism in two-dimensional (2D) van der Waals materials have provided a new platform for the study of magnetic semiconductors [4]. The Ising ferromagnetism with out-of-plane magnetization was observed in monolayer CrI_3 in experiment with $T_c = 45$ K [5]. The Heisenberg ferromagnetic state was obtained in 2D $\text{Cr}_2\text{Ge}_2\text{Te}_6$ in experiment with $T_c = 28$ K in bilayer $\text{Cr}_2\text{Ge}_2\text{Te}_6$ [6], where the corresponding bulk was known as a layered ferromagnet with spin along c axis and $T_c = 61$ K in experiment [7]. A large remanent magnetization with out-of-plane magnetic anisotropy was recently reported in experiment in the 6-nm film of $\text{Cr}_2\text{Ge}_2\text{Te}_6$ on a topological insulator $(\text{Bi,Sb})_2\text{Te}_3$ with $T_c = 80$ K [8]. The magnetic structure in monolayer CrI_3 and $\text{Cr}_2\text{Ge}_2\text{Te}_6$ was recently discussed in terms of Kitaev interaction [9]. Photoluminescence and magneto-optical effects have also been discussed [10, 11]. The ferromagnetism with high T_c was also reported in experiment in the monolayer VSe_2 [12] and MnSe_2 [13]. Despite the relatively small number of monolayer ferromagnetic materials realized in experiment, predicting promising candidates by first principles calculations can provide reliable reference for experiments [14, 15]. Researchers have also studied possible

2D ferromagnetic materials by machine learning [16] and high-throughput calculations [17].

Several methods are used to control the magnetic states in these recently discovered 2D materials. By tuning gate voltage, the switching between antiferromagnetic and ferromagnetic states in bilayer CrI_3 was obtained in experiment [18]. Using gate voltage, the enhancement of ferromagnetism in 2D Fe_3GeTe_2 was observed in recent experiment [19]. In 2D transition metal dichalcogenides, which are non-magnetic, the strain is used to modify the optical and electronics properties [20]. The effect of strain is studied to affect the ferromagnetism in monolayer $\text{Cr}_2\text{Ge}_2\text{Te}_6$ [21] and CrX_3 ($X = \text{Cl}, \text{Br}, \text{I}$) [22]. The electric field effect was discussed in experiment in magnetic multilayer $\text{Cr}_2\text{Ge}_2\text{Te}_6$ [23]. Recently, heterostructures of these 2D materials have also been studied [24–26].

In this paper, by density functional theory calculations we predict a stable 2D ferromagnetic semiconductor $\text{Cr}_2\text{Ge}_2\text{Se}_6$. We find that $T_c = 144$ K in $\text{Cr}_2\text{Ge}_2\text{Se}_6$, which can be enhanced to $T_c = 326$ K by applying 3% strain, and $T_c = 421$ K by 5% strain. On the other hand, T_c in 2D semiconductor $\text{Cr}_2\text{Ge}_2\text{Te}_6$ is about 30 K in our calculation, close to the value of $T_c = 28$ K in recent experiment [6]. In addition, the anomalous Hall conductivity in 2D $\text{Cr}_2\text{Ge}_2\text{Se}_6$ and $\text{Cr}_2\text{Ge}_2\text{Te}_6$ is predicted to be comparable to that in ferromagnetic metals of Fe and Ni [27–29], and is an order of magnitude larger than that in diluted magnetic semiconductor Ga(Mn,As) [30, 31]. The strain is found to decrease the energy difference between $3d$ orbitals of Cr and $4p$ orbitals of Se, which induces the enhanced ferromagnetic coupling based on the superexchange picture. Our finding highlights the microscopic mechanism to obtain the room temperature magnetic semiconductors by strain.

* gubo@ucas.ac.cn

† gsu@ucas.ac.cn

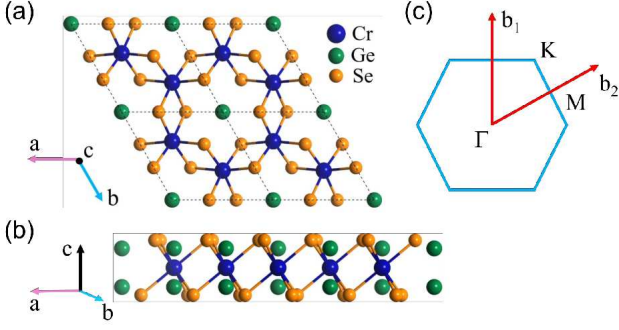


FIG. 1. Crystal structure of $\text{Cr}_2\text{Ge}_2\text{Se}_6$ of (a) top view in a-b plane and (b) side view in a-c plane. The two-dimensional Brillouin zone is shown in (c).

II. CALCULATION METHODS

The density functional theory (DFT) calculations are done by the Vienna *ab initio* simulation package (VASP) [32]. The spin-polarized calculation with projector augmented wave (PAW) method, and general gradient approximations (GGA) in the Perdew-Burke-Ernzerhof (PBE) exchange correlation functional are used. The spin-orbit coupling (SOC) is included in the calculations. Total energies are obtained with k-grids $9 \times 9 \times 1$ by Mohnkhorst-Pack approach. The lattice constants and atom coordinates are optimized with the energy convergence less than 10^{-6} eV and the force less than 0.01 eV/Å, where a large vacuum of 20 Å is used to model a 2D system. The phonon calculations are performed with density functional perturbation theory (DFPT) by the PHONOPY code [33]. Size of the supercell is $3 \times 3 \times 1$, where the displacement is taken by 0.01 Å.

For the on-site Coulomb interaction U of Cr ion, the values in range of 3 ~ 5 eV are usually reasonable for 3d transition metal insulators [34], while a small value of $U < 2$ eV was adopted in the DFT calculation of 2D $\text{Cr}_2\text{Ge}_2\text{Te}_6$ [6]. We fixed the parameter $U = 4$ eV in most of our following calculations for 2D $\text{Cr}_2\text{Ge}_2\text{Te}_6$ and $\text{Cr}_2\text{Ge}_2\text{Se}_6$, and will discuss the effect of different U parameters later.

Based on the DFT results, the Curie temperature is calculated by using the Monte Carlo simulations[21, 22] based on the 2D Ising model, where a 60×60 supercell is adopted, and 10^5 steps are performed for every temperature to acquire the equilibrium. The anomalous Hall conductivity is calculated with Wannier90 code [35] and WannierTools code [36].

III. CRYSTAL STABILITY

We study the stability of the 2D new material $\text{Cr}_2\text{Ge}_2\text{Se}_6$. We propose this material guided by the recently reported 2D material $\text{Cr}_2\text{Ge}_2\text{Te}_6$ in experiment, and we replace Te by Se. The crystal structure of

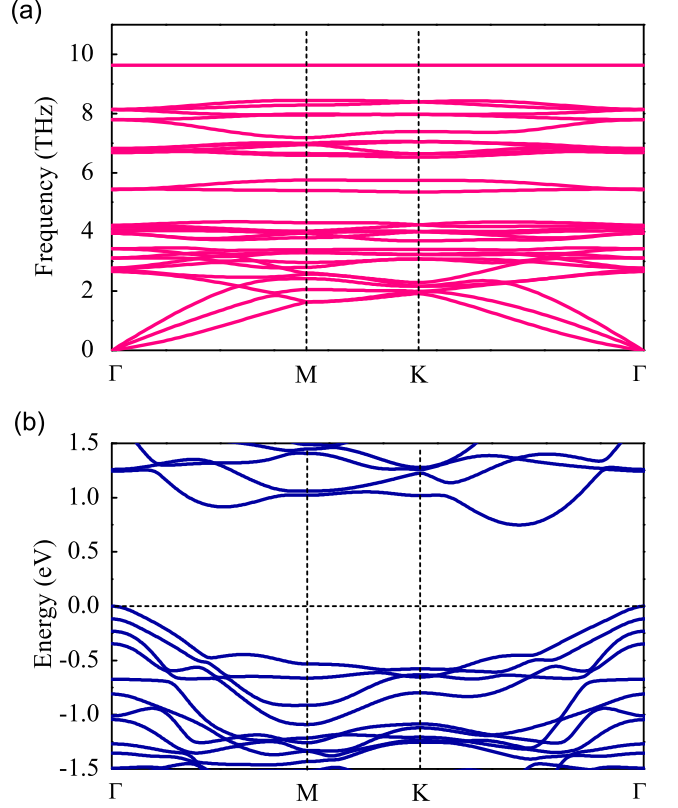


FIG. 2. (a) Phonon spectrum and (b) electron band structure of two-dimensional $\text{Cr}_2\text{Ge}_2\text{Se}_6$, obtained by the spin-polarized GGA + SOC + U calculations.

$\text{Cr}_2\text{Ge}_2\text{Se}_6$ is shown in Fig. 1 (a) for top view and 1 (b) for side view, where the space group number is 162 (P-31m). The structure is obtained by the fully relaxed calculation. The optimized lattice constant of 2D $\text{Cr}_2\text{Ge}_2\text{Se}_6$ is calculated as 6.413 Å, which is smaller than the lattice constant 6.8275 Å of $\text{Cr}_2\text{Ge}_2\text{Te}_6$ in experiment. It is reasonable because Se has a smaller radius than Te. We examine the stability in terms of phonon spectrum, where the Brillouin zone is shown in Fig. 1(c). As shown in Fig. 2(a), there is no imaginary frequency in the phonon dispersion near Γ point. It predicts that the crystal structure of monolayer $\text{Cr}_2\text{Ge}_2\text{Se}_6$ is stable.

To further check the crystal stability, we study the formation energy of monolayer $\text{Cr}_2\text{Ge}_2\text{Se}_6$ and $\text{Cr}_2\text{Ge}_2\text{Te}_6$ by DFT calculations. The formation energy of $\text{Cr}_2\text{Ge}_2\text{Se}_6$ is given by $E_{\text{form}} = E_{\text{tot}} - 2E_{\text{Cr}} - 2E_{\text{Ge}} - 6E_{\text{Se}}$, where E_{tot} is the total energy of the 2D $\text{Cr}_2\text{Ge}_2\text{Se}_6$, and E_{Cr} , E_{Ge} and E_{Se} are the total energy per atom for the bulk chromium, germanium and selenium, respectively. We found that the formation energy of monolayer $\text{Cr}_2\text{Ge}_2\text{Se}_6$ is -1.13 eV, lower than the 0.92 eV of monolayer $\text{Cr}_2\text{Ge}_2\text{Te}_6$. It suggests that the 2D $\text{Cr}_2\text{Ge}_2\text{Se}_6$ should be more stable than 2D $\text{Cr}_2\text{Ge}_2\text{Te}_6$, the latter was realized in recent experiment [6].

The electronic band structure of $\text{Cr}_2\text{Ge}_2\text{Se}_6$ is shown in Fig. 2(b). An indirect band gap of 0.748 eV is observed,

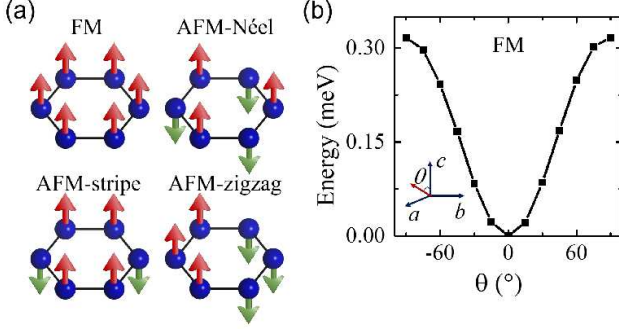


FIG. 3. (a) Four possible states for two-dimensional $\text{Cr}_2\text{Ge}_2\text{Se}_6$: ferromagnetic (FM) state, antiferromagnetic (AFM) Néel state, AFM stripe state, and AFM zigzag state. Balls denote Cr atoms, and arrows denote spins. (b) Total energy as a function of angle θ for the FM state, obtained by the spin-polarized GGA + SOC + U calculations.

and monolayer $\text{Cr}_2\text{Ge}_2\text{Se}_6$ is a semiconductor. Recently, it has been found that the change of the magnetization direction can alter the band structures in 2D CrI_3 [37]. In our case, we calculate the band structure of $\text{Cr}_2\text{Ge}_2\text{Se}_6$ with the in-plane magnetization, and find that the band structure does not change dramatically. In addition, we uncover that a larger band gap of 1.38 eV is obtained by using the HSE06 hybrid functional, whereas the profiles of band structure do not change.

IV. MAGNETIC PROPERTIES

To study the magnetic ground state of 2D $\text{Cr}_2\text{Ge}_2\text{Se}_6$, we examine the possible states with paramagnetic, ferromagnetic and antiferromagnetic configurations. The calculations reveal that the energy of the paramagnetic state is 6 eV higher than the ferromagnetic and antiferromagnetic states. Fig. 3(a) shows four possible magnetic states of 2D $\text{Cr}_2\text{Ge}_2\text{Se}_6$: ferromagnetic (FM) state, antiferromagnetic (AFM) Néel state, AFM stripe state, and AFM zigzag state. The calculations show that the FM state is the most stable state, and the energy difference between the FM and the AFM configuration is more than 30 meV as listed in Table I. Furthermore, as shown in Fig. 3(b), the calculations show that the lowest energy of ferromagnetic state is obtained when the magnetization direction is perpendicular to the two-dimensional materials, with magnetic anisotropy energy of 0.32 meV per unit cell of $\text{Cr}_2\text{Ge}_2\text{Se}_6$. As listed in Table I, the calculation shows that for 2D $\text{Cr}_2\text{Ge}_2\text{Se}_6$, the spin momentum of Cr atom is $3.4 \mu_B$, and the occupation number of Cr 3d orbitals is 3.976.

The Curie temperature T_c can be estimated by the Monte Carlo simulation based on a 2D Ising model. The exchange coupling parameter is estimated as the total energy difference of ferromagnetic and antiferromagnetic states $E^{\text{AFM}} - E^{\text{FM}}$ as listed in Table I, which was ob-

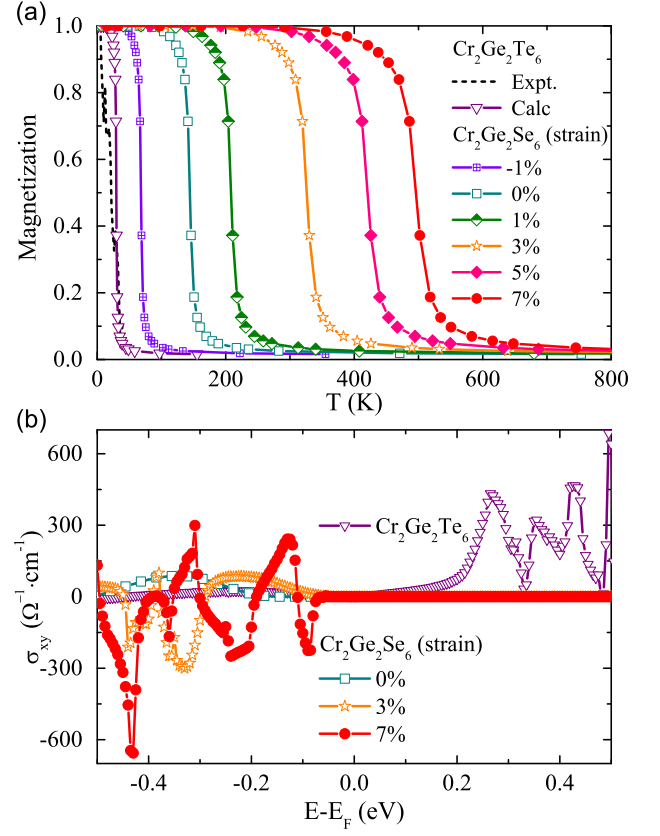


FIG. 4. For two-dimensional $\text{Cr}_2\text{Ge}_2\text{Te}_6$ and $\text{Cr}_2\text{Ge}_2\text{Se}_6$ with different strains, (a) the normalized magnetization as a function of temperature, and (b) the anomalous Hall conductivity as a function of energy. The experimental result of $\text{Cr}_2\text{Ge}_2\text{Te}_6$ is taken from Ref. [6]. The calculation results are obtained by the DFT calculations and Monte Carlo simulations.

TABLE I. For 2D semiconductor $\text{Cr}_2\text{Ge}_2\text{Te}_6$, $\text{Cr}_2\text{Ge}_2\text{Se}_6$, and $\text{Cr}_2\text{Ge}_2\text{Se}_6$ with 5% strain, DFT results of total energy of ferromagnetic state E^{FM} , total energy of antiferromagnetic state E^{AFM} , Curie temperature T_c , 3d orbital occupation number n_d , spin (S) and orbital (L) momentum of Cr atom, and bond length $d_{\text{Cr-Te/Se}}$.

DFT	$\text{Cr}_2\text{Ge}_2\text{Te}_6$	$\text{Cr}_2\text{Ge}_2\text{Se}_6$	
		no strain	5% strain
$E^{\text{FM}}(\text{eV})$	-89.1376	-97.3460	-96.5658
$E^{\text{AFM}}(\text{eV})$	-89.1309	-97.3135	-96.4710
$E^{\text{AFM}} - E^{\text{FM}}(\text{meV})$	6.7	32.5	98.8
$T_c(\text{K})$	30	144	421
$n_d(\text{Cr})$	4.043	3.976	3.951
$S(\mu_B)(\text{Cr})$	3.586	3.404	3.487
$L(\mu_B)(\text{Cr})$	-0.018	-0.076	-0.105
$d_{\text{Cr-Te/Se}}(\text{\AA})$	2.827	2.64	2.697

tained by the DFT calculations. The obtained normalized magnetization as function of temperature is shown in Fig. 4 (a). The experimental result of magnetization for $\text{Cr}_2\text{Ge}_2\text{Te}_6$ is taken from temperature-dependent Kerr rotation of bilayer $\text{Cr}_2\text{Ge}_2\text{Te}_6$ with $T_c = 28$ K [6]. The calculated Curie temperature is $T_c = 30$ K for the monolayer $\text{Cr}_2\text{Ge}_2\text{Te}_6$, which is close to the experimental value. It is noted that for simplicity the Ising model is applied in our Monte Carlo simulation, while the Heisenberg model with magnetic anisotropy was suggested in experiment [6]. In addition, the estimated Curie temperature T_c could be even larger by using the mean field approximation [17]. The calculated Curie temperature for monolayer $\text{Cr}_2\text{Ge}_2\text{Se}_6$ is $T_c = 144$ K, which is about 5 times higher than the $T_c = 30$ K for monolayer $\text{Cr}_2\text{Ge}_2\text{Te}_6$ by the Monte Carlo simulation. More interestingly, the Curie temperature can be enhanced to $T_c = 326$ K by applying tensile 3% strain, and $T_c = 421$ K with 5% strain. We find that T_c is decreased to 67 K with 1% compression strain, as shown in Fig. 4(a), and the system becomes antiferromagnetic when applying 2% compression strain. Our result predicts that monolayer $\text{Cr}_2\text{Ge}_2\text{Se}_6$ by applying a few percent tensile strain can be a promising candidate for room-temperature ferromagnetic semiconductor.

As the magnetization direction is out-of-plane with an easy axis along c direction in 2D $\text{Cr}_2\text{Ge}_2\text{Te}_6$ and $\text{Cr}_2\text{Ge}_2\text{Se}_6$, it is interesting to study the anomalous Hall conductivity due to the Berry curvature of band structure. By the DFT calculations, the results are shown in Fig. 4(b). The magnitude of anomalous Hall conductivity σ_{xy} for the p-type $\text{Cr}_2\text{Ge}_2\text{Se}_6$ and n-type $\text{Cr}_2\text{Ge}_2\text{Te}_6$ can be as large as 4×10^2 ($\Omega \text{ cm}$) $^{-1}$. This value is comparable to the σ_{xy} in some ferromagnetic metals, such as $\sigma_{xy} = 7.5 \times 10^2$ in bcc Fe [27, 28], and $\sigma_{xy} = 4.8 \times 10^2$ ($\Omega \text{ cm}$) $^{-1}$ in fcc Ni [29] due to the Berry curvature of band structures. More importantly, the estimated σ_{xy} in 2D magnetic semiconductors $\text{Cr}_2\text{Ge}_2\text{Te}_6$ and $\text{Cr}_2\text{Ge}_2\text{Se}_6$ is an order of magnitude larger than the σ_{xy} of classic diluted magnetic semiconductor Ga(Mn,As) [30, 31].

V. DISCUSSION

To study the effect of the on-site Coulomb interaction U of $3d$ orbitals of Cr, we calculate the Curie temperature T_c as a function of parameter U for 2D $\text{Cr}_2\text{Ge}_2\text{Te}_6$, $\text{Cr}_2\text{Ge}_2\text{Se}_6$ without strain and with 5% strain, as shown in Fig. 5. The experimental T_c of 2D $\text{Cr}_2\text{Ge}_2\text{Te}_6$ is taken from Ref. [6]. For 2D $\text{Cr}_2\text{Ge}_2\text{Te}_6$, the calculated T_c is decreased with increasing U , and close to the experimental T_c with $U = 4$ eV. In addition, we found that the magnetization direction of $\text{Cr}_2\text{Ge}_2\text{Te}_6$ becomes in-plane with $U = 1$ eV, which disagrees with experiment. The antiferromagnetic ground state is obtained for $\text{Cr}_2\text{Ge}_2\text{Te}_6$ with $U = 5$ eV, which is also against with the experiment. Our calculations suggest that the reasonable U for 2D $\text{Cr}_2\text{Ge}_2\text{Te}_6$ may be in the range of $2 \sim 4$ eV.

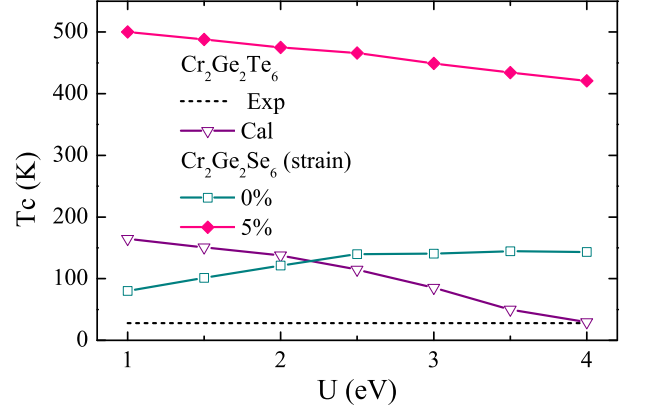


FIG. 5. The Curie temperature T_c as a function of parameter U for 2D $\text{Cr}_2\text{Ge}_2\text{Te}_6$, $\text{Cr}_2\text{Ge}_2\text{Se}_6$ without strain and with 5% strain. The experimental result of $\text{Cr}_2\text{Ge}_2\text{Te}_6$ and the calculations are the same in Fig. 4(a), except with different values of U .

TABLE II. For 2D semiconductor $\text{Cr}_2\text{Ge}_2\text{Se}_6$ without strain and with 5% strain, DFT results of hopping matrix element $|V|$ and energy difference $|E_p - E_d|$ between $4p$ orbitals of Se and $3d$ orbitals of Cr.

strain	hopping matrix element $ V $ (eV)				
	$p_z-d_{z^2}$	p_z-d_{xz}	p_z-d_{yz}	$p_z-d_{x^2-y^2}$	p_z-d_{xy}
0%	0.257983	0.29527	0.380283	0.190041	0.445906
5%	0.258289	0.22747	0.306872	0.201524	0.416315
	energy difference $ E_p - E_d $ (eV)				
	$p_z-d_{z^2}$	p_z-d_{xz}	p_z-d_{yz}	$p_z-d_{x^2-y^2}$	p_z-d_{xy}
0%	1.415092	0.4458	0.45512	0.581666	0.581166
5%	1.552237	0.09143	0.09775	0.695055	0.693946

For 2D $\text{Cr}_2\text{Ge}_2\text{Se}_6$ with 5% strain, the calculated T_c is always higher than room temperature with parameter U in the range of $1 \sim 4$ eV, as shown in Fig. 5. Thus, our prediction about the room temperature ferromagnetic semiconductor $\text{Cr}_2\text{Ge}_2\text{Se}_6$ with a few percent strain is robust with the values of parameter U .

How to understand the enhancement of T_c in 2D $\text{Cr}_2\text{Ge}_2\text{Se}_6$ by applying strain? According to the superexchange interaction [38–40], the FM coupling is expected since the Cr-Se-Cr bond angle is close to 90 degree. The indirect FM coupling between Cr atoms is proportional to the direct AFM coupling between neighboring Cr and Se atom. The magnitude of this direct AFM coupling can be roughly estimated as $J = \frac{|V|^2}{|E_p - E_d|}$, where $|V|$ is the hopping matrix element between $4p$ orbitals of Se and $3d$ orbitals of Cr, and $|E_p - E_d|$ is the energy difference between $4p$ orbitals of Se and $3d$ orbitals of Cr. By DFT calculations, we can obtain these parameters for 2D $\text{Cr}_2\text{Ge}_2\text{Se}_6$ without strain and with 5% strain. The results of $|V|$ and $|E_p - E_d|$ are listed in Table II. The results suggest that the strain has little effect on the

hopping $|V|$, while the strain can make energy difference between p_z orbital of Se and d_{xz} and d_{yz} orbitals of Cr decreased to one-fifth of the value without strain, causing a dramatical enhancement of the AFM coupling between Cr and Se atom. This leads to the enhanced FM coupling between Cr atoms, and makes T_c beyond the room temperature.

VI. SUMMARY

By the DFT calculations we predict a stable 2D ferromagnetic semiconductor $\text{Cr}_2\text{Ge}_2\text{Se}_6$. We find the Curie temperature T_c of $\text{Cr}_2\text{Ge}_2\text{Se}_6$ can be dramatically enhanced beyond room temperature by applying 3% strain, which is much higher than the $T_c = 28$ K in 2D $\text{Cr}_2\text{Ge}_2\text{Te}_6$ in recent experiment. In addition, the anomalous Hall conductivity in 2D $\text{Cr}_2\text{Ge}_2\text{Se}_6$ and $\text{Cr}_2\text{Ge}_2\text{Te}_6$ is predicted to be an order of magnitude larger than that in diluted magnetic semiconductor $\text{Ga}(\text{Mn},\text{As})$. Based

on the superexchange interaction, the decreased energy difference between $4p$ orbitals of Se and $3d$ orbitals of Cr is found to be important to enhance the T_c in 2D $\text{Cr}_2\text{Ge}_2\text{Se}_6$ by applying strain. Our finding highlights the microscopic mechanism to obtain the room temperature ferromagnetic semiconductors by strain.

ACKNOWLEDGMENTS

The authors acknowledge Q. B. Yan, Z. G. Zhu, and Z. C. Wang for many valuable discussions. BG is supported by NSFC(Grant No. Y81Z01A1A9), CAS (Grant No.Y929013EA2) and UCAS (Grant No.110200M208). GS is supported in part by the the National Key R&D Program of China (Grant No. 2018FYA0305800), the Strategic Priority Research Program of CAS (Grant Nos.XDB28000000, XBD07010100), the NSFC (Grant No.11834014), and Beijing Municipal Science and Technology Commission (Grant No. Z118100004218001).

-
- [1] H. Ohno, Making nonmagnetic semiconductors ferromagnetic, *Science* **281**, 951 (1998).
 - [2] T. Dietl, A ten-year perspective on dilute magnetic semiconductors and oxides, *Nat. Mater.* **9**, 965 (2010).
 - [3] L. Chen, X. Yang, F. Yang, J. Zhao, J. Misuraca, P. Xiong, and S. von Molnár, Enhancing the curie temperature of ferromagnetic semiconductor $(\text{Ga},\text{Mn})\text{As}$ to 200 K via nanostructure engineering, *Nano Lett.* **11**, 2584 (2011).
 - [4] K. S. Burch, D. Mandrus, and J.-G. Park, Magnetism in two-dimensional van der Waals materials, *Nature* **563**, 47 (2018).
 - [5] B. Huang, G. Clark, E. Navarro-Moratalla, D. R. Klein, R. Cheng, K. L. Seyler, D. Zhong, E. Schmidgall, M. A. McGuire, D. H. Cobden, W. Yao, D. Xiao, P. Jarillo-Herrero, and X. Xu, Layer-dependent ferromagnetism in a van der Waals crystal down to the monolayer limit, *Nature* **546**, 270 (2017).
 - [6] C. Gong, L. Li, Z. Li, H. Ji, A. Stern, Y. Xia, T. Cao, W. Bao, C. Wang, Y. Wang, Z. Q. Qiu, R. J. Cava, S. G. Louie, J. Xia, and X. Zhang, Discovery of intrinsic ferromagnetism in two-dimensional van der Waals crystals, *Nature* **546**, 265 (2017).
 - [7] V. Cartheaux, D. Brunet, G. Ouvrard, and G. Andre, Crystallographic, magnetic and electronic structures of a new layered ferromagnetic compound $\text{Cr}_2\text{Ge}_2\text{Te}_6$, *J. Phys.: Condens. Matter* **7**, 69 (1995).
 - [8] M. Mogi, A. Tsukazaki, Y. Kaneko, R. Yoshimi, K. S. Takahashi, M. Kawasaki, and Y. Tokura, Ferromagnetic insulator $\text{Cr}_2\text{Ge}_2\text{Te}_6$ thin films with perpendicular remanence, *APL Mater.* **6**, 091104 (2018).
 - [9] C. Xu, J. Feng, H. Xiang, and L. Bellaiche, Interplay between kitaev interaction and single ion anisotropy in ferromagnetic CrI_3 and CrGeTe_3 monolayers, *npj Comput. Mater.* **4**, 57 (2018).
 - [10] K. L. Seyler, D. Zhong, D. R. Klein, S. Gao, X. Zhang, B. Huang, E. Navarro-Moratalla, L. Yang, D. H. Cobden, M. A. McGuire, W. Yao, D. Xiao, P. Jarillo-Herrero, and X. Xu, Ligand-field helical luminescence in a 2D ferromagnetic insulator, *Nat. Phys.* **14**, 277 (2017).
 - [11] Y. Fang, S. Wu, Z.-Z. Zhu, and G.-Y. Guo, Large magneto-optical effects and magnetic anisotropy energy in two-dimensional $\text{Cr}_2\text{Ge}_2\text{Te}_6$, *Phys. Rev. B* **98**, 125416 (2018).
 - [12] M. Bonilla, S. Kolekar, Y. Ma, H. C. Diaz, V. Kalappattil, R. Das, T. Eggers, H. R. Gutierrez, M.-H. Phan, and M. Batzill, Strong room-temperature ferromagnetism in VSe_2 monolayers on van der Waals substrates, *Nat. Nanotech.* **13**, 289 (2018).
 - [13] D. J. O'Hara, T. Zhu, A. H. Trout, A. S. Ahmed, Y. K. Luo, C. H. Lee, M. R. Brenner, S. Rajan, J. A. Gupta, D. W. McComb, and R. K. Kawakami, Room temperature intrinsic ferromagnetism in epitaxial manganese selenide films in the monolayer limit, *Nano Lett.* **18**, 3125 (2018).
 - [14] B. Shabbir, M. Nadeem, Z. Dai, M. S. Fuhrer, Q.-K. Xue, X. Wang, and Q. Bao, Long range intrinsic ferromagnetism in two dimensional materials and dissipationless future technologies, *Appl. Phys. Rev.* **5**, 041105 (2018).
 - [15] N. Sivasdas, M. W. Daniels, R. H. Swendsen, S. Okamoto, and D. Xiao, Magnetic ground state of semiconducting transition-metal trichalcogenide monolayers, *Phys. Rev. B* **91**, 235425 (2015).
 - [16] T. D. Rhone, W. Chen, S. Desai, A. Yacoby, and E. Kaxiras, Data-driven studies of magnetic two-dimensional materials, arXiv preprint arXiv:1806.07989 (2018).
 - [17] H. Liu, J.-T. Sun, M. Liu, and S. Meng, Screening magnetic two-dimensional atomic crystals with nontrivial electronic topology, *J. Phys. Chem. Lett.* **9**, 6709 (2018).
 - [18] B. Huang, G. Clark, D. R. Klein, D. MacNeill, E. Navarro-Moratalla, K. L. Seyler, N. Wilson, M. A. McGuire, D. H. Cobden, D. Xiao, W. Yao, P. Jarillo-Herrero, and X. Xu, Electrical control of 2D magnetism in bilayer CrI_3 , *Nat. Nanotech.* **13**, 544 (2018).

- [19] Y. Deng, Y. Yu, Y. Song, J. Zhang, N. Z. Wang, Z. Sun, Y. Yi, Y. Z. Wu, S. Wu, J. Zhu, J. Wang, X. H. Chen, and Y. Zhang, Gate-tunable room-temperature ferromagnetism in two-dimensional Fe_3GeTe_2 , *Nature* **563**, 94 (2018).
- [20] R. Roldán, A. Castellanos-Gomez, E. Cappelluti, and F. Guinea, Strain engineering in semiconducting two-dimensional crystals, *J. Phys.: Condens. Matter* **27**, 313201 (2015).
- [21] X. Li and J. Yang, CrXTe_3 ($X = \text{Si, Ge}$) nanosheets: two dimensional intrinsic ferromagnetic semiconductors, *J. Mater. Chem. C* **2**, 7071 (2014).
- [22] J. Liu, Q. Sun, Y. Kawazoe, and P. Jena, Exfoliating biocompatible ferromagnetic Cr-trihalide monolayers, *Phys. Chem. Chem. Phys.* **18**, 8777 (2016).
- [23] W. Xing, Y. Chen, P. M. Odenthal, X. Zhang, W. Yuan, T. Su, Q. Song, T. Wang, J. Zhong, S. Jia, X. C. Xie, Y. Li, and W. Han, Electric field effect in multilayer $\text{Cr}_2\text{Ge}_2\text{Te}_6$: a ferromagnetic 2D material, *2D Mater.* **4**, 024009 (2017).
- [24] D. Zhong, K. L. Seyler, X. Linpeng, R. Cheng, N. Sivadas, B. Huang, E. Schmidgall, T. Taniguchi, K. Watanabe, M. A. McGuire, W. Yao, D. Xiao, K.-M. C. Fu, and X. Xu, Van der Waals engineering of ferromagnetic semiconductor heterostructures for spin and valleytronics, *Sci. Adv.* **3**, e1603113 (2017).
- [25] Z. Wang, T. Zhang, M. Ding, B. Dong, Y. Li, M. Chen, X. Li, J. Huang, H. Wang, X. Zhao, Y. Li, D. Li, C. Jia, L. Sun, H. Guo, Y. Ye, D. Sun, Y. Chen, T. Yang, J. Zhang, S. Ono, Z. Han, and Z. Zhang, Electric-field control of magnetism in a few-layered van der Waals ferromagnetic semiconductor, *Nat. Nanotech.* **13**, 554 (2018).
- [26] M. Lohmann, T. Su, B. Niu, Y. Hou, M. Alghamdi, M. Aldosary, W. Xing, J. Zhong, S. Jia, W. Han, R. Wu, Y.-T. Cui, and J. Shi, Probing magnetism in insulating $\text{Cr}_2\text{Ge}_2\text{Te}_6$ by induced anomalous Hall effect in Pt, *Nano Lett.* **19**, 2397 (2019).
- [27] Y. Yao, L. Kleinman, A. H. MacDonald, J. Sinova, T. Jungwirth, D. Sheng Wang, E. Wang, and Q. Niu, First principles calculation of anomalous Hall conductivity in ferromagnetic bcc Fe, *Phys. Rev. Lett.* **92**, 037204 (2004).
- [28] X. Wang, J. R. Yates, I. Souza, and D. Vanderbilt, Ab initio calculation of the anomalous Hall conductivity by wannier interpolation, *Phys. Rev. B* **74**, 195118 (2006).
- [29] X. Wang, D. Vanderbilt, J. R. Yates, and I. Souza, Fermi-surface calculation of the anomalous Hall conductivity, *Phys. Rev. B* **76**, 195109 (2007).
- [30] T. Jungwirth, J. Sinova, K. Y. Wang, K. W. Edmonds, R. P. Campion, B. L. Gallagher, C. T. Foxon, Q. Niu, and A. H. MacDonald, Dc-transport properties of ferromagnetic (Ga,Mn)As semiconductors, *Appl. Phys. Lett.* **83**, 320 (2003).
- [31] J. Sinova, T. Jungwirth, S.-R. E. Yang, J. Kučera, and A. H. MacDonald, Infrared conductivity of metallic (III,Mn)V ferromagnets, *Phys. Rev. B* **66**, 041202 (2002).
- [32] G. Kresse and J. Furthmüller, Efficient iterative schemes for ab initio total-energy calculations using a plane-wave basis set, *Phys. Rev. B* **54**, 11169 (1996).
- [33] A. Togo and I. Tanaka, First principles phonon calculations in materials science, *Scr. Mater.* **108**, 1 (2015).
- [34] S. Maekawa, T. Tohyama, S. E. Barnes, S. Ishihara, W. Koshibae, and G. Khaliullin, *Physics of Transition Metal Oxides* (Springer Berlin Heidelberg, 2004), Series in Solid State Sciences, Vol. 144.
- [35] A. A. Mostofi, J. R. Yates, G. Pizzi, Y.-S. Lee, I. Souza, D. Vanderbilt, and N. Marzari, An updated version of wannier90: A tool for obtaining maximally-localised wannier functions, *Comput. Phys. Commun.* **185**, 2309 (2014).
- [36] Q. Wu, S. Zhang, H.-F. Song, M. Troyer, and A. A. Soluyanov, WannierTools: An open-source software package for novel topological materials, *Comput. Phys. Commun.* **224**, 405 (2018).
- [37] P. Jiang, L. Li, Z. Liao, Y. X. Zhao, and Z. Zhong, Spin direction-controlled electronic band structure in two-dimensional ferromagnetic CrI_3 , *Nano Lett.* **18**, 3844 (2018).
- [38] J. B. Goodenough, Theory of the role of covalence in the perovskite-type manganites $[\text{La, M(II)}]\text{MnO}_3$, *Phys. Rev.* **100**, 564 (1955).
- [39] J. Kanamori, Crystal distortion in magnetic compounds, *J. Appl. Phys.* **31**, S14 (1960).
- [40] P. W. Anderson, New approach to the theory of superexchange interactions, *Phys. Rev.* **115**, 2 (1959).